Thermodynamic and Structural Effects of a Single Backbone Hydrogen Bond Deletion in a Metal-Assembled Helical Bundle Protein

Jian Zhou,[†] Martin A. Case,[†] James F. Wishart,[‡] and George L. McLendon*,[†]

Department of Chemistry, Princeton University, Princeton, New Jersey 08544, and Chemistry Department, Brookhaven National Laboratory, Upton, New York 11973

Received: July 2, 1998; In Final Form: October 8, 1998

Transition metal ion-assembled three-helix bundle proteins provide templates to investigate the thermodynamic and dynamic structural consequences of the deletion of a single backbone hydrogen bond from an α-helical architecture. This deletion does not perturb the steady-state secondary structure of the protein as measured by circular dichroism spectroscopy but does decrease the overall folding free energy by ca. 0.7 kcal/mol. We have used intraprotein electron transfer as a measure of the structure-sensitive dynamics of our system. The deletion of a single hydrogen bond in one of the helices of a three-helix bundle does not significantly change the measured electron-transfer rate. This is in agreement with "Greenpath" electron-transfer pathway calculations, which assume a constant and invariant structure for the architecture. Given the exponential dependence of electron-transfer rate on distance and that fluctuations in the intervening secondary structure will cause variations in electron donor−acceptor distances, the measured electron-transfer rate associated with hydrogen bond deletion allows us to calculate a differential dynamic structural fluctuation associated with hydrogen bond deletion of less than 0.6 Å over the millisecond time scale of the experiment.

Introduction

The de novo design of proteins is a field of research no longer in its infancy. Several motifs have been designed from first principles using a range of approaches including synthetic self-assembly,[1] combinatorial genetics,[2] and directed computer-aided design.[3]

Given this level of success, it becomes possible to embark on the predictive design of function for proteins[4] and to probe the roles of specific interactions in order to better understand protein structure, stability, and functionality. The contribution of protein backbone hydrogen bonds to the processes of protein folding and stabilization has received extensive theoretical investigation,[5] but to date, there has been little experimental validation of theory.[6] As far as we are aware, there has been no investigation of the influence of backbone hydrogen bonding on the *dynamic* stability of proteins.

Clearly, when aspects of protein structure, which require chemical compromise of the amide backbone, are investigated, the customary tools of site-directed mutagenesis are not expected to serve us well. The only biomimetic approach to have shown success when applied to the analysis of backbone amide hydrogen bonding has been the unnatural amino acid mutagenesis approach pioneered by Schultz, in which the tRNA amber suppressor is hijacked to expand the repertoire of amino acids available to in vivo protein synthesis machinery.[6] Although this strategy has been successful, it remains technically challenging. Total protein synthesis offers the advantage that the backbone of the protein can be altered at will simply by incorporating artificial amino acid analogues into a solid-phase peptide synthesis protocol. The principal drawback is that the maximum length for a polypeptide chain synthesized by state-of-the-art solid-phase methodology is on the order of 100 amino acids. Although the techniques of native chemical ligation[7] offer enormous potential in this area, the simpler approach of metal ion-assisted assembly of synthetically tractable peptide subunits can provide architectures that possess the structural attributes of natural proteins in a more straightforward manner.[1c−f] Of the common protein structural motifs, helical bundles offer a combination of flexibility in design, freedom from intermolecular interactions in solution, and spectroscopic accessibility for the purposes of analysis. We therefore adopted this motif to examine the effects of a single backbone hydrogen bond deletion on the steady state and dynamic stability and structure of a parallel three-helix bundle.

Previously, we have shown that a compact, globular, parallel three-helix bundle synthesized by metal-ion assisted assembly offers a free energy of stabilization of folding of up to 4 kcal/mol and that the unfolding transition is reasonably cooperative.[1f] Extensive thermodynamic analysis of similar systems implicates hydrophobic collapse of amphipathic helices as the main driving force for folding.[1a,c−f] The individual helices are designed to present a hydrophobic, leucine-rich "stripe" along the length of the helix when folded, and each helix possesses an N-terminal bidentate metal-binding ligand (a 2,2′-bipyridyl derivative). Sequestration of three such ligands by a six-coordinate metal ion serves to reduce the translational and rotational entropy of the system, allowing hydrophobic collapse of the architecture to a parallel, in-register three-helix bundle. We speculated that the free energy of folding of an analogous parallel three-helix bundle in which only two of the helices have an intact hydrogen-bonding network should be sufficient to induce the folding of the third, parallel, in-register helix, even though this third helix is missing one part of its hydrogen-bonding network and would be expected to be less stable than either of the two supporting helices.

The deletion of a single hydrogen bond may be achieved by substituting one amide bond in the backbone of one of the

[†] Princeton University.
[‡] Brookhaven National Laboratory.

10.1021/jp982852f CCC: $15.00
Published on Web 12/03/1998

Figure 1. Model of three-helix bundle metalloprotein. α-Helices are shown as ribbons. The backbone hydrogen bonding residues and the ruthenium tris(bipyridine) moiety are shown in ball-and-stick representation.[23]

α-helices with an ester bond, thus disrupting the hydrogen bond between this amide proton at position $i + 4$ and the carbonyl group of the backbone of the amino acid at position i (Figure 1).

Comparisons of the steady-state structures and stabilities of such designed proteins may be afforded by circular dichroism spectroscopy[8] and thermal or chemical denaturation studies, respectively.[9] Assessment of the contributions of dynamic flexibility to the stabilities of these systems, however, presents more of a challenge.

The growing consensus correlating protein structure with intramolecular protein electron-transfer rates suggests that the comparative electron-transfer rates of the intact three-helix bundle, and the isosteric system with a single hydrogen bond excised, might provide a sensitive dynamic structural probe.[10] The electron-transfer rate constant depends exponentially on the electron donor−acceptor distance, and thus, in principle, such rates should be far more sensitive reporters of distance than traditional (Förster) energy-transfer methods. Furthermore, the electron-transfer approach may be able to probe a wider dynamic range than energy transfer. To assess the dynamic structural fluctuations associated with hydrogen bond excision, we used pulse radiolysis to determine the intramolecular electron-transfer rate between two redox-active metal centers, between which we engineered the hydrogen bond deletion. The metal ion complex, which serves as the sequestrant for the assembly process, may be introduced as one-half of a redox couple for electron-transfer studies. The redox partner is attached to the helix under investigation such that the backbone hydrogen bond of interest (or the hydrogen bond deletion) lies between the electron donor and acceptor.

Here, we report comparative electron-transfer rates as a probe for the dynamic structural comparisons of two systems, which differ by one backbone hydrogen bond. To our knowledge, this is the first such application of electron transfer as a "dynamic ruler".

Materials and Methods

Unless otherwise stated, reagents were purchased from Aldrich Chemical Co. (Milwaukee, WI) or Fisher Scientific (Pittsburgh, PA) and used without further purification. Methylbenzhydrylamine (MBHA) solid-phase peptide synthesis resin, Fmoc, and ^{t}Boc-protected amino acids were obtained from Advanced ChemTech (Louisville, KY) and NovaBiochem (San Diego, CA). The detailed description of solid-phase peptide synthesis (SPPS) and purification has been described elsewhere.[11] Ruthenium(II) hexakis(dimethyl sulfoxide), $[Ru(DMSO)_6](NO_3)_2$, was synthesized according to literature procedures.[12] Composition of each product was assessed by UV−visible spectroscopy, electrospray mass spectrometry, and analytical HPLC. The concentrations of peptides and metallopeptides were determined according to their UV−visible spectra: $\lambda = 290$ nm ($\epsilon = 1.2 \times 10^4$) for bipyridyl peptides, $\lambda = 290$ nm ($\epsilon = 3.2 \times 10^4$) for bis(bipyridyl)metallopeptides, and $\lambda = 472$ nm ($\epsilon = 1.15 \times 10^3$) for tris(bipyridyl)-metallopeptides. Circular dichroism spectra were recorded on an Aviv 62DS CD spectrometer at 20 °C with a bandwidth of 0.5 nm in degassed sodium borate buffer (25 mM, pH 7.0). $Ru(NH_3)_5$-modified metalloproteins were synthesized according to published procedures with modifications described in the text.[13] Pulse radiolysis measurements were performed at Brookhaven National Laboratory.[14] The radiolysis samples were prepared in a cocktail comprising sodium phosphate buffer (10 mM, pH 7.0), *tert*-butyl alcohol (1 M), and $NaClO_4$ (50 mM) under Ar. The absorbance change at 380 nm was monitored for the disappearance of the radiolytically formed $Ru[(bpy)_2(bpy^-)]^{2+}$ species.

Synthesis of *tert*-Butyl (*S*)-(+)-5-Oxo-2-tetrahydrofurancarboxylate (1). To a solution of (*S*)-(+)-5-oxo-2-tetrahydrofurancarboxylic acid (3.00 g, 23 mmol) in dichloromethane (20 mL) was added a solution consisting of dicyclohexylcarbodiimide (DCC, 0.523 g, 25.4 mmol) and 4-pyrrolidinopyridine (PDP, 0.340 g, 23.1 mmol) in dichloromethane (5 mL). The solution was stirred at room temperature for 30 min. To this solution was added a solution of *tert*-butyl alcohol (1.88 g, 25.4 mmol) in dichloromethane (5 mL), and the reaction was continued for a further hour. The solid remaining after removal of solvent in vacuo was taken up in a mixture of diethyl ether and hexane (1:1). Filtration of this suspension followed by evaporation of the filtrate to dryness resulted in pure product. Yield: 3.2 g, 75%. ^{1}H NMR (DMSO-d_6): δ 4.93 (CH_2), 3.32 (CH), 2.12 (CH_2), 1.39 [$C(CH_3)_3$].

Synthesis of *tert*-Butyl L-1-Amido-4-hydroxy-5-pentanedioate (2). To solid **1** (1 g, 5.37 mmol) was added slowly aqueous NH_3 (5 mL, sp gr 0.880). The reaction was kept at room temperature for 5 h, after which the solvent was removed in vacuo. The crude solid was recrystallized from a mixture of diethyl ether and hexane (1:1). Yield: 1 g, 91%. ^{1}H NMR (DMSO-d_6): δ 7.28, 6.78 (NH), 5.20 (CH_2), 3.90 (CH), 2.10 (CH_2), 1.41 [$C(CH_3)_3$].

Synthesis of Fmoc-leu*gln-O^{t}Bu (3). To a solution of **2** (0.480 g, 2.36 mmol) in dichloromethane (5 mL) was added a solution of DCC (0.536 g, 2.60 mmol), PDP (0.035 g, 0.236 mmol), and Fmoc-leu-OH (0.92 g, 2.60 mmol). After the solution was stirred at room temperature for 4 h, the solvent was removed and the resulting solid was taken up in a mixture of ether and hexane (10 mL, 3:1). The resulting suspension was filtered, the filtrate collected, and precipitation of the

product induced by the addition of hexane (50 mL). Yield: 1.17 g, 92%. The product was characterized by mass spectroscopy (observed, 538; calculated, 538) and ^{1}H NMR.

Synthesis of Fmoc-leu*gln-OH (4). To solid **3** (0.300 g, 0.557 mmol) was added TFA (1 mL), and after 1 h the reaction mixture was pumped dry. The resulting solid was washed with hexane (10 mL) and a mixture of ethyl ether and hexane (1:1). The crude product was recrystallized from diethyl ether. Yield: 240 mg, 90%. The product was characterized by mass spectroscopy and ^{1}H NMR.

Synthesis of α*p* and α*p*9H. These peptides were synthesized on MBHA resin (0.72 mmol/g, 0.64 g) using a ^{t}Boc SPPS protocol. Coupling of residues was performed using ^{t}Boc-protected amino acids activated by HBTU/DIEA in DMF. Deprotection of the ^{t}Boc groups was by TFA. The terminal 4-carboxy-2,2′-bipyridine was attached using HBTU/DIEA in DMF. The peptides were deprotected and cleaved from the resin using liquid HF (1 h, 0 °C, 10 mL/g resin) with anisole as scavenger (10% v/v). The crude peptides were precipitated with ice-cold diethyl ether, taken up in dilute acetic acid (5%), and lyophilized to dryness. Crude peptides were purified using preparative reverse-phase HPLC and characterized by analytical HPLC and electrospray mass spectroscopy.

Synthesis of α*p*9H*. The peptide was synthesized on MBHA resin (0.72 mmol/g, 0.64 g) using a combination of ^{t}Boc and Fmoc SPPS protocols. Coupling of residues 20−9 was performed using ^{t}Boc-protected amino acids activated by HBTU/DIEA in DMF. Deprotection of the ^{t}Boc groups was by TFA. The dipeptide isostere **4** was coupled to the free amino terminus of the supported peptide using HBTU/DIEA in DMF. Deprotection of the Fmoc group was effected using two treatments with piperidine (10 min, 50% in DMF). Residues 6−1 were coupled using ^{t}Boc strategy. The terminal 4-carboxy-2,2′-bipyridine was attached using HBTU/DIEA in DMF. The peptide was deprotected and cleaved from the resin using liquid HF (1 h, 0 °C, 10 mL/g resin) with anisole as scavenger (10% v/v). The crude peptide was precipitated with ice-cold diethyl ether, taken up in dilute acetic acid (5%), and lyophilized to dryness. The crude peptide was purified using preparative reverse-phase HPLC and characterized by analytical HPLC and electrospray mass spectroscopy.

Synthesis of [Ru(α*p*)$_2$(solvent)$_2$]. An amount of 2 equiv of α*p* peptide (21 mg, 8.58 μmol) in water (1 mL) was added to a solution of Ru(DMSO)$_6$(NO$_3$)$_2$ (50 μL, 85 μmol/mL) in a mixture of water (1 mL) and DMSO (0.1 mL). The solution was slowly warmed to 80 °C, and the reaction was continued for 30 min. The product was purified by reverse-phase HPLC on a semipreparative C-18 column with a linear gradient of 45−55% *i*-PrOH/water solvent system containing 0.1% TFA over 40 min. Those peaks with a mass spectrum indicative of the Ru(α*p*)$_2$ species were collected and pooled. Yield: 13.1 mg, 60%. The major byproduct was identified as Ru(α*p*)$_3$. Product confirmation was by analytical reverse-phase HPLC and electrospray mass spectroscopy (calculated, 4996; observed, 4997).

Synthesis of Mixed Three-Helix Bundles: [Ru(α*p*)$_2$(α*p*9H)]$^{2+}$ and [Ru(α*p*)$_2$(α*p*9H*)]$^{2+}$. A solution of the respective peptide (α*p*9H or α*p*9H*, 4 equiv) in water (1 mL) was added to a solution of [Ru(α*p*)$_2$(solvent)$_2$] in water (1 mL) at 80 °C. The reaction was allowed to continue at 80 °C for 50 min. The products were purified using reverse-phase HPLC eluted with 40%−60% CH$_3$CN/H$_2$O buffer containing 0.1% TFA and characterized by electrospray mass spectroscopy. The yields of these mixed three-helix bundles are quantitative.

Synthesis of Ruthenium(II) Pentammine Derivatives of Three-Helix Bundles: [Ru(α*p*)$_2$(α*p*9H)]$^{2+}$−[Ru(NH$_3$)$_5$]$^{3+}$ and [Ru(α*p*)$_2$(α*p*9H*)]$^{2+}$−[Ru(NH$_3$)$_5$]$^{3+}$. Ruthenium(II) pentammine was prepared by quantitative reduction of [Ru(NH$_3$)$_5$Cl]Cl$_2$ in HEPES buffer (100 mM, pH 7) over a freshly prepared Zn/Hg amalgam. To avoid decomposition of the Ru(II) species, the reduced pentammine was used as soon as dissolution of the starting material was complete (room temperature, 15−20 min). The solution of Ru(II) pentammine (1 mL, 50-fold excess) was filtered through a 0.2 μm nylon syringe filter directly onto the lyophilized metalloprotein (5 mg) and the reaction mixture stirred under Ar (room temperature, 1 h). It should be noted that a study of the time course of an analogous reaction by HPLC indicated that unwanted byproducts were formed in substantial quantities after 2 h. The crude mixture was oxidized by passing O$_2$ through the solution; unreacted Ru(II) pentammine was oxidized to Ru(III) pentammine derivatives and precipitated accordingly. The oxidized metalloprotein adduct remained as an orange solution. The pure product was isolated by size-exclusion chromatography on Sephadex G25 (Pharmacia, Piscataway NJ) with elution by sodium phosphate buffer (50 mM, pH 7). The yields of ruthenium(III) pentammine adducts were quantitative.

Buffer exchanges for circular dichroism and pulse radiolysis studies were effected by size-exclusion chromatography on Sephadex G25 with elution by the appropriate buffer.

Results and Discussion

Design and Syntheses. Amino acid sequences of the consensus peptide (α*p*), the helix with intact hydrogen bond (α*p*9H), and the helix with the hydrogen bond deletion (α*p*9H*) are as follows:

α*p*: bpy-gly-glu-leu-ala-gln-lys-leu-glu-gln-ala-leu-gln-lys-leu-glu-gln-ala-leu-gln-lys-amide

α*p*9H: bpy-gly-glu-leu-ala-gln-lys-**leu-gln**-his-ala-leu-gln-lys-leu-glu-gln-ala-leu-gln-lys-amide

α*p*9H*: bpy-gly-glu-leu-ala-gln-lys-**leu*gln**-his-ala-leu-gln-lys-leu-glu-gln-ala-leu-gln-lys-amide

where bpy is 5-carboxy-2,2′-bipyridine and **leu*gln** is the ester formed from L-leucine and L-1-amido,4-hydroxypentanedioic acid (the alcohol analogue of L-glutamine).

The rationale for the consensus sequence, α*p*, has been described in detail elsewhere.[1d−f] The histidine residues at positions 9 in the sequences α*p*9H and α*p*9H* serve as attachment sites for [Ru(NH$_3$)$_5$]$^{3+}$ electron acceptor groups.[13] Upon attachment, the sixth ligand site of the ruthenium pentammine is occupied by the ε-nitrogen of the histidine imidazole moiety.

The two constructs employed in these studies were assembled using a novel heterotrimeric synthesis of the ruthenium(II) complexes Ru[(α*p*)$_2$(α*p*9H)]$^{2+}$ and Ru[(α*p*)$_2$(α*p*9H*)]$^{2+}$. Steady-state secondary structures of the constructs were analyzed using circular dichroism spectroscopy. Relative stabilities of the proteins were inferred from measurements of the free energies of folding as measured by chemical denaturation and extrapolation to zero denaturant concentration. The molecules are hyperthermophilic[15] and are therefore not amenable to thermal denaturation.

The ester isostere of the leu-gln dipeptide was introduced into the peptide by standard solid-phase peptide synthesis. The rationale for substitution of glutamine at position 8 in peptides

αp9H and αp9H*, for glutamic acid in the consensus sequence αp, was for synthetic reasons. There was a possibility for intramolecular transesterification if the glutamic acid side chain remained. The incorporation of the ester bond in the peptide was demonstrated by 2D ^{1}H NMR studies. A "NOESY walk" was performed through the Cα and NH protons until the ester was reached, at the expected position. Mass spectroscopic results confirmed that no cleavage of the peptide had occurred.

To replace only one hydrogen bond in the 60 amino acid construct, it was necessary to create a mixed helix bundle in which only one of three peptides contained the ester isostere. The synthesis of such mixed ruthenium three-helix bundles presents a synthetic challenge. Although the synthesis of homotrimeric three-helix bundles is usually achieved by the reaction of excess peptide with metal ions,[1d−f] this approach is not applicable to the synthesis of a mixed bundle system. When a mixture of two equivalents of αp and one equivalent of αp9H* was reacted with substoichiometric "ruthenium blue[16]", a convenient source of Ru(II), the yield of the desired mixed bundle [Ru(αp)$_2$(αp9H*)] was less than 5% because of the greater thermodynamic stability of the homotrimeric [Ru(αp)$_3$]$^{2+}$. A two-step reaction scheme was conceived in order to address this difficulty. The problem is twofold. First, a source of ruthenium(II) must be chosen that allows the reaction to be stopped at the homodimeric stage, [Ru(αp)$_2$(solvent)$_2$]$^{2+}$. Second, the ligand system of the ruthenium(II) must be sufficiently labile to permit the thermodynamic equilibration necessary to guarantee that the homodimer adopts the more stable (and structurally desirable) facial geometry at the metal center. It was found that ruthenium(II) hexakis(dimethyl sulfoxide), [Ru(DMSO)$_6$]$^{2+}$, fulfilled both these criteria. The [Ru(αp)$_2$(solvent)$_2$]$^{2+}$ two-helix bundle is moderately stable in dilute solution and can be purified by reverse-phase HPLC. Acetonitrile must be avoided as eluent because of its high affinity for the remaining sites on the ruthenium(II) bis(bipyridyl) complex. Rapid lyophilization of the purified material is essential if disproportionation to [Ru(αp)$_3$]$^{2+}$ is to be avoided.

The syntheses of mixed three-helix bundles from [Ru(αp)$_2$(solvent)$_2$]$^{2+}$ are straightforward. Reaction with 4- to 5-fold excess of the third helix went to completion within 50 min at 80 °C. The products [Ru(αp)$_2$(αp9H)]$^{2+}$ and [Ru(αp)$_2$(αp9H*)]$^{2+}$ were purified by reverse-phase HPLC and product identities confirmed by electrospray mass spectrometry. Analytical reverse-phase HPLC and circular dichroism spectroscopy indicate that the products consist of two facial diastereoisomers, with 50% each of ΔL and ΛL stereochemistries. The Δ/Λ nomenclature describes the stereochemistry at the ruthenium(II) tris(bipyridine) center, and the L nomenclature refers to the stereochemistry of the amino acids and hence the right-handed pitch of the α-helices. The observation of diastereomers in the synthesis of this class of molecules is consistent with the results of previous work.[1f] Stability measurements and pulse radiolysis experiments were performed on a racemic mixture of ΔL and ΛL diastereoisomers.

Steady-State Conformational Analysis. Although there remains some controversy over the extent of stabilization,[5,17] it is certainly true that α-helices are stabilized in part by backbone hydrogen bonds. Given these uncertainties, it is not intuitively obvious to what degree the static or dynamic structure of the three-helix bundle system should be perturbed by deletion of an isolated hydrogen bond.

Circular dichroism spectroscopy provides a simple and robust measure of the α-helical content of protein structure (although with some caveats[18]) and is particularly suited as a tool for comparison of the two homologous structures [Ru(αp)$_2$(αp9H)]$^{2+}$ and [Ru(αp)$_2$(αp9H*)]$^{2+}$. The two systems have identical circular dichroism spectra and thus appear to have identical static secondary structure. The amplitude of the 222 nm negative ellipticity suggests that both proteins, with and without the backbone amide bond, are approximately 90% helical. The steady-state circular dichroism spectra are presented in Figure 2.

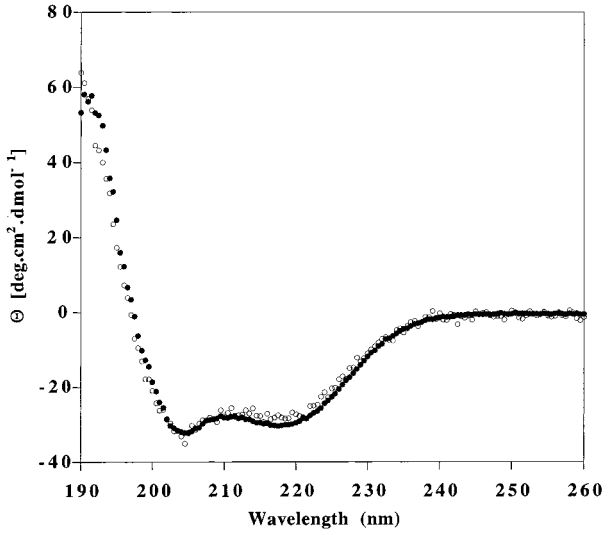

Figure 2. CD spectra of three-helix bundle metalloproteins: (●) [Ru(*ap*)$_2$(*ap*9H)]; (○) [Ru(*ap*)$_2$(*ap*9H*)]. Experimental conditions are given in the text.

Thermodynamic Analysis of Folding. Although the static secondary structure appears unaltered by the hydrogen bond deletion, the circular dichroism experiment does not address the thermodynamic consequences of such a modification. To explore this, reversible equilibrium unfolding of metalloproteins was performed. Unfolding was induced by addition of the chaotropic agent guanidinium hydrochloride. Unfolding was monitored by following the characteristic 222 nm ellipticity, which is indicative of the helical content of the protein.

Both proteins exhibit cooperative chemical denaturation as illustrated in Figure 3. The cooperativity parameter, as measured by the slope of the unfolding curve in the region where log(K_{app}) is proportional to denaturant concentration, is similar for both systems; however, the midpoint of the unfolding transition is shifted to lower denaturant concentration when the backbone hydrogen bond is deleted. A quantitative analysis of these data, extrapolated to zero denaturant concentration, suggests that the specific backbone hydrogen bond between residues 5 and 9 contributes $\Delta\Delta G = 0.7$ kcal/mol to the total stability of the folded helix bundle relative to an unfolded reference state. It should be noted that this value does not solely represent the strength of an intrahelical amide bond.[6b] For comparison, the $\Delta\Delta G$s for backbone hydrogen bond deletions at the N-terminus of an α-helix (residues 39−50 of T4 lysozyme[6b]), at the C-terminus of the same helix,[6b] and in an antiparallel β-sheet (staphylococcal nuclease[6c]) are reported to be 0.9, 0.7, and 2.5 kcal/mol, respectively. It seems reasonable that the lower values for the α-helix backbone are largely due to the solvent accessibility of this motif. In this context, the $\Delta\Delta G$ value of 0.7 kcal/mol measured in this work seems reasonable. Although this is slightly less than a comparable solvent-shielded backbone hydrogen bond in T4 lysozyme,[6b] it

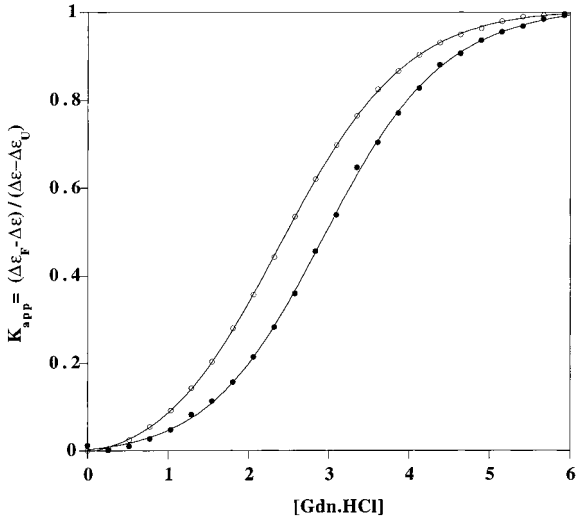

Figure 3. Denaturation of three-helix bundle metalloproteins: guanidinium hydrochloride denaturation of [Ru(*ap*)$_2$(*ap*9H)] (●); [Ru(*ap*)$_2$(*ap*9H*)] (○). K_{app} was determined from the change in ellipticity at 222 nm. Experimental conditions are given in the text.

is expected when one considers the molten globule nature of our constructs and thus their inherently greater solvent accessibility.

Dynamic Conformational Analysis: Electron Transfer as a Structural Probe. The equilibrium thermodynamic consequences for the folding of this specific backbone hydrogen bond deleted protein are significant; 0.7 kcal/mol represents some 30% of the free energy of folding of the protein with intact backbone hydrogen bonds. The value of 0.7 kcal/mol agrees broadly with results from other studies in which side chain internal hydrogen bonds have been excised by mutagenesis, although it is somewhat low compared to the values obtained in other backbone hydrogen bond deletion studies. The modest cooperativity of unfolding in these helical bundles supports the contention that the 0.7 kcal/mol change represents a substantial fraction of the total free energy for folding. Although the static structure as measured by circular dichroism spectroscopy does not appear to be dependent on the presence or absence of the backbone hydrogen bond in question, such destabilization might be expected to result in an increase of the frequency and/or amplitude of protein structural fluctuations—the "breathing" of the protein. Such fluctuations, when observed in natural proteins, have been shown to have significant effects on reactivity.[19] To address this question, we sought a functional probe that could reveal, with high sensitivity, such dynamic fluctuations.

Over the past decade, work from many groups has established the factors that dictate the dependence of protein electron-transfer rate on the distance between an electron donor and acceptor. The roles of specific pathways in such processes have been explored extensively at both a theoretical[20] and an experimental level.[10a,21] It has become clear that for a broad class of molecules, from small molecules in organic solvents to proteins in aqueous environments, electron-transfer rate constants scale well with the distance-dependent tunneling matrix elements and generally follow an exponential dependence:

$$k_{ET} \propto \exp(-\beta R)$$

where k_{ET} is the electron-transfer rate constant, R is the distance between the electron donor and acceptor, and β is the electronic

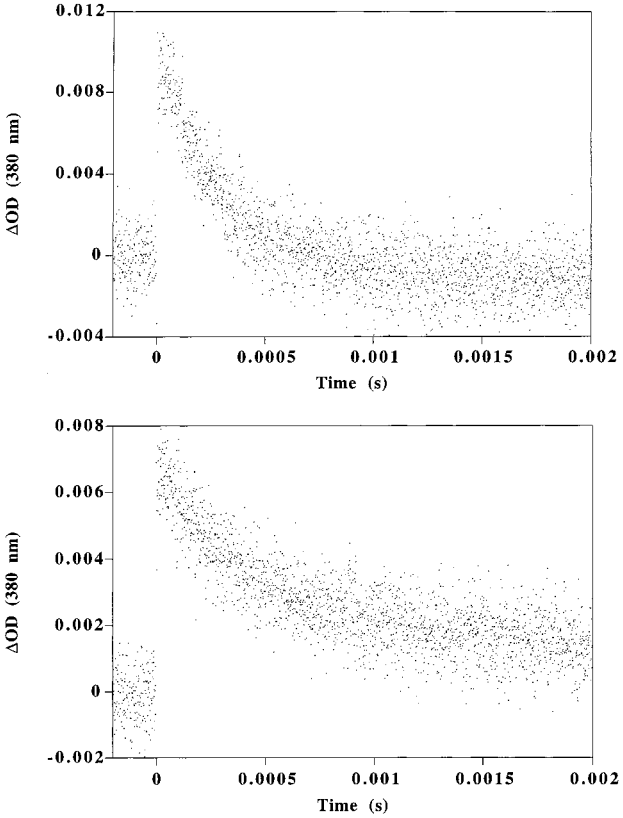

Figure 4. Pulse radiolysis data: (top) [Ru(*ap*)$_2$(*ap*9H)]; (bottom) [Ru(*ap*)$_2$(*ap*9H*)]. Disappearance of Ru[(bpy)$_2$(bpy$^-$)]$^{2+}$ species was monitored by the absorbance change at 380 nm. Experimental conditions are given in the text.

damping factor. The proportionality constant in this equation is the Franck−Condon weighted density of states and is dependent on the reorganization energy and the driving force of the electron-transfer process. These terms are the same for the two systems under investigation.

We have examined the distance dependence of electron transfer in this class of three-helix bundles[22] and found that $\beta = 1.2$ Å^{-1}. It follows that if, for example, hydrogen bond deletion resulted in an average change in donor−acceptor distance of 2 Å, the measured electron-transfer rate would be expected to change by an order of magnitude. It is this exponential dependence of rate on distance that makes electron transfer potentially a very sensitive way to monitor small structure changes. Because of this sensitivity to distance, small fluctuations in structure, which increase the donor−acceptor distance, should alter the measured electron-transfer rate observably. The electron-transfer rates from the ruthenium(II) tris(bipyridyl) moiety to the ruthenium(III) pentaammine appended to the imidazole group of the histidine residue at position 9 were measured by pulse radiolysis. Representative traces are shown in Figure 4.

It was found that deletion of the hydrogen bond results in a very modest change in the observed electron-transfer rate:

$$k_{ET}[\mathrm{Ru}(\alpha p)2(\alpha p9\mathrm{H})] = 3 \times 10^3\ \mathrm{s}^{-1}$$

$$k_{ET}[\mathrm{Ru}(\alpha p)2(\alpha p9\mathrm{H}^*)] = 2 \times 10^3\ \mathrm{s}^{-1}$$

Such a difference might arise from fluctuations in structure or from differences in the electron-transfer pathway, since hydrogen bonds are believed to play a crucial role in mediating the

pathways for electron transfer. Pathway calculations suggest that the hydrogen bond excised does not lie on a major pathway for electron transfer. This in itself is an interesting result, since it suggests that there is apparently a single, dominant pathway (at least in calculations) even in such simple constructs. Assuming that the dominant pathway for electron transfer does not involve the deleted backbone hydrogen bond, we may calculate the maximum structural change associated with the hydrogen bond deletion to be $\Delta R \leq 0.6$ Å over the millisecond time scale of the measurement.

It is pertinent to ask what resolution we might expect of this technique. The estimated errors in the calculation of k_{ET} by pulse radiolysis are approximately 20%, largely due to uncertainty in the intrinsic decay rate of the bipyridyl ligand-centered radical species. Thus, $\Delta R = 0.3 \pm 0.3$ Å and the expected resolution of this technique is approximately 0.5 Å. The distance over which the electron-transfer rates were measured in these systems is calculated to be 20 Å. By use of techniques of electron-transfer rate measurements such as picosecond pulse radiolysis or flash photolysis, distances as short as 5 Å may be measured.

Conclusions

It is now possible to design and create proteins that adopt predictable structures. These structures may be chemically altered to probe fundamental questions of structure and function. In the present work, a backbone hydrogen bond in a protein α-helix was chemically deleted, and the effects of this alteration on stability monitored. A stability change of $\Delta\Delta G = 0.7$ kcal/mol was assigned to this hydrogen bond. These structures can also provide functional templates for introducing reactivity into proteins. The dependence of electron-transfer rate on distance, although very sensitive, is also predictable and robust. The sensitivity of electron-transfer rate to structure suggests that electron transfer may be used in special situations to probe structure change. The present work presents, to the best of our knowledge, the first report of a dynamic structural comparison between two proteins measured by electron transfer. Given the sensitivity of this technique to small structural changes, it is hoped that other applications may emerge.

Acknowledgment. This paper is dedicated to Professor Bard, a pioneer in electron-transfer studies (and an indefatigable doubles partner). Preliminary support for this work was provided by NIH (GM33881-12). Primary and continuing support is provided by NSF Division of Chemistry (CHE-9729124). This research was carried out in part at Brookhaven National Laboratory under Contract DE-AC02-98CH10886 with the U.S. Department of Energy and supported by its Division of Chemical Sciences, Office of Basic Energy Sciences.

References and Notes

(1) (a) Tuchscherer, G.; Mutter, M. *Pure Appl. Chem*. **1996**, *68*, 2153. (b) Dawson, P. E.; Kent, S. B. H. *J. Am. Chem. Soc*. **1993**, *115*, 7263. (c) Lieberman, M.; Sasaki, T. *J. Am. Chem. Soc.* **1991**, *113*, 1470. (d) Ghadiri, M. R.; Soares, C.; Choi, C. *J. Am. Chem. Soc.* **1992**, *114*, 825. (e) Ghadiri, M. R.; Case, M. A. *Angew. Chem., Int. Ed. Engl.* **1993**, *32*, 1594. (f) Case M. A.; Mutz M. W.; McLendon, G. L. *Chirality* **1998**, *10*, 35.

(2) (a) Eisenberg, D.; Wilcox, W.; Eshita, S. M.; Pryciak, P. M.; Ho, S. P.; DeGrado, W. F. *Proteins* **1986**, *1*, 16. (b) Zhao, H. M.; Arnold, F. H. *Curr. Opin. Struct. Biol.* **1997**, *7*, 480. (c) Beasley, J. R.; Hecht, M. H. *J. Biol. Chem*. **1997**, *272*, 2031 and references therein.

(3) (a) Dahiyat, B. I.; Mayo, S. L. *Science* **1997**, *278*, 82. (b) Hellinga, H. W.; Caradonna, J. P.; Richards, F. M. *J. Mol. Biol*. **1991**, *222*, 787. (c) Hurley, J. H.; Baase, W. A.; Matthews, B. W. *J. Mol. Biol*. **1992**, *224*, 1143. (d) Betz, S. F.; Degrado, W. F. *Biochemistry* **1996**, *35*, 6955. (e) Desjarlais, J. R.; Handel, T. M. *Protein Sci*. **1995**, *4*, 2006. (f) Harbury, P. B.; Tidoe, B.; Kim, P. S. *Proc. Natl. Acad. Sci. U.S.A.* **1995**, *92*, 8408. (g) Roberson, D. E.; Farid, R. S.; Moser, C. C.; Urbauer, J. L.; Mulholland, S. E.; Pidikiti, R.; Lear, J. D.; Wand, A. J.; Degrado, W. F.; Dutton, P. L. *Nature* **1994**, *368*, 425.

(4) Tuchscherer, G.; Scheilber, L.; Dumy, P.; Mutter, M. *Biopolymers* **1998**, *47*, 63.

(5) (a) Dill, K. A. *Biochemistry* **1990**, *29*, 7133. (b) Doig, A. J.; Williams, D. H. *J. Am. Chem. Soc*. **1992**, *114*, 338. (c) Honig, B.; Yang, A.-S. *Adv. Protein Chem*. **1995**, *46*, 27. (d) Murphy, K. P.; Gill, S. J. *J. Mol. Biol*. **1991**, *222*, 699.

(6) (a) Shin, I.; Ting, A. Y.; Schultz, P. G. *J. Am. Chem. Soc*. **1997**, *119*, 12667. (b) Koh, J. T.; Cornish, V. W.; Schultz, P. G. *Biochemistry* **1997**, *36*, 11314. (c) Chapman, E.; Thorson, J. S.; Schultz, P. G. *J. Am. Chem. Soc*. **1997**, *119*, 7151.

(7) Lu, W.; Qasim, M. A.; Laskowski, M., Jr.; Kent, S. H. B. *Biochemistry* **1997**, *36*, 673.

(8) Cantor, C. R.; Schimmel, P. R. In *Biophysical Chemistry, Part II*; W. H. Freeman and Company: New York, 1980.

(9) Pace, C. N.; Vanderburg, K. E. *Biochemistry* **1979**, *18*, 288.

(10) (a) Gray, H. B.; Winkler, J. R. *Annu. Rev. Biochem.* **1996**, *65*, 537. (b) Mocek, H. M.; Zhou, J. S.; Forest, S. D.; Priyadarshy, S.; Beratan, D. N.; Onuchic, J. N.; Hoffman, B. M. *Chem. Rev*. **1996**, *96*, 2459. (c) Marcus, R. A.; Sutin, N. *Biochim. Biophys. Acta* **1985**, *811*, 265. (d) Beratan, N. M.; Onuchic, J. N. *Electron Transfer in Inorganic, Organic, and Biological Systems*; American Chemical Society: Washington, DC, 1991; Vol. 228. (e) McLendon, G. L. *Electron Transfer Proteins*; Marcel Dekker: New York, 1995. (f) McLendon, G. L.; Simolo, K.; Magner, E.; Taylor, K.; Guarr, T.; McGuire, M.; Miller, J. Proceedings of Pacific Basins Symposium on Photochemistry of Inorganic Compounds. *Coord. Chem. Rev*. **1985**.

(11) (a) Stewart, J. M.; Young, J. D. *Solid Phase Peptide Synthesis*; Pierce Chemical Co.: Rockford, IL, 1984. (b) Schnolzer, M.; Alewood, P.; Jones, A.; Alewood, D.; Kent, S. B. H. *Int. J. Pept. Protein Res*. **1992**, *40*, 180.

(12) Davis, A. R.; Einstein, F. W. B.; Farrell, N. P.; James, B. R.; McMillan, R. S. *Inorg. Chem*. **1978**, *17*, 1965.

(13) (a) Yocom, K. M.; B., S. J.; Shelton, J. R.; E., S. W.; G., W. *Proc. Natl. Acad. Sci. U.S.A.* **1982**, *79*, 7052. (b) Matthews, C. R.; Erickson, P. M.; Van Vliet, D. L.; Petersheim, M. *J. Am. Chem. Soc.* **1978**, *100*, 2260. (c) Dahiyat, B.; Meade, T. J.; Mayo, S. L. *Inorg. Chim. Acta* **1996**, *243*, 207.

(14) (a) Vassilian, A.; Wishart, J. F.; van Hemelryck, B.; Schwarz, H.; Isied, S. S. *J. Am. Chem. Soc*. **1990**, *112*, 7278. (b) Ogawa, M. Y.; Wishart, J. F.; Young, Z.; Miller, J. R.; Isied, S. S. *J. Phys. Chem*. **1993**, *97*, 11456.

(15) Jiang X.; Bishop, E. J.; Farid R. S. *J. Am. Chem. Soc*. **1997**, *119*, 838.

(16) Rose, D.; Wilkinson, G. *J. Chem. Soc. A.* **1970**, 1791.

(17) Creighton, T. E. *Curr. Biol*. **1991**, *1*, 5.

(18) Miick, S. M.; Martinez, G. V.; Fiori, W. R.; Todd, A. P.; Millhauser, G. L. *Nature* **1992**, *359*, 653; **1995**, *377*, 257.

(19) (a) Morgan, B. P.; Scholtz, J. M.; Ballinger, M. D.; Zipkin, I. D.; Bartlett, P. A. *J. Am. Chem. Soc.* **1991**, *113*, 297. (b) Bugg, T. D. H.; Wright, G. D.; Dutka-Malen, S.; Arthur, M.; Courvalin, P.; Walsh, C. T. *Biochemistry* **1991**, *30*, 10408. (c) Groeger, C.; Wenzel, H. R.; Tshesche, H. *Int. J. Pept. Protein Res*. **1994**, *44*, 166.

(20) (a) Beratan, D. N.; Onuchic, J. N.; Winkler, J. R.; Gray, H. B. *Science* **1992**, *258*, 1740. (b) Beratan, D. N.; Betts, J. N.; Onuchic, J. N. *J. Phys. Chem*. **1992**, *96*, 2852.

(21) (a) Langen, R.; Colon J. L.; Casimiro, D. R.; Karpishin, T. B.; Winkler, J. R.; Gray, H. B. *J. Biol. Inorg. Chem.* **1996**, *1*, 221. (b) Wuttke, D. S.; Bjerrum, M. J.; Winkler, J. R.; Gray, H. B. *Science* **1992**, *256*, 1007. (c) Langen, R.; Chang, I. J.; Germanas, J. P.; Richards, J. H.; Winkler, J. R.; Gray, H. B. *Science* **1995**, *268*, 1733.

(22) Mutz, M. W.; Case, M. A.; Wishart, J. F.; Ghadiri, M. R.; McLendon, G. L. *J. Am. Chem. Soc*., in press.

(23) Kraulis, P. J. *J. Appl. Crystallogr*. **1991**, *24*, 946.